Mecánica Computacional Vol. XXI, pp. 1382–1401
S. R. Idelsohn, V. E. Sonzogni and A. Cardona (Eds.)
Santa Fe–Paraná, Argentina, October 2002

ERROR INDICATOR FOR MIXED FINITE ELEMENTS

Cyntia G. da Costa*, and Lavinia M.S.A. Borges*

*Laboratory of Solid Mechanics
Federal University of Rio de Janeiro, PEM/COPPE
P.O.Box: 68503, zip: 21945-970, Rio de Janeiro, RJ, Brazil
e-mails: cyntia@mecsol.ufrj.br and lavinia@ufrj.br

Key Words: Error Estimator, Mixed Formulation, Finite Element Method, Thermo–elasticity, Incompressible Materials.

Abstract. *The main objective of this paper is to propose an "a posteriori"error indicator and a finite element adaptive strategy for the Reissner-Hellinger thermo–elasticity formulation. The paper presents triangular finite elements with quadratic and continuous displacements interpolation and discontinuous stress interpolation. Two different interpolations for the stress field are considered. In plane stress condition, total stress is linearly interpolated. Likewise, the deviatoric stress is regarded as linear for plane strain and under symmetry of revolution conditions but the mean stress is considered to be constant in each element. These mixed elements are appropriated for facing the locking phenomena when incompressibility is presented. The proposed error indicator is based on second-order derivatives of the Mises equivalent stress and mean stress associated with a recovered stress field. That is, gradients and/or Hessians of the stress solution, obtained on a given mesh, are smoothed and then used in the error estimation. The error indicator is related with the maximum eigenvalue of such Hessians. Some numerical examples are presented in order to show the viability of this adaptive mesh refinement and to compare its performance with the error estimates found in literature.*

1 INTRODUCTION

This paper aims to propose an *a posteriori* error indicator and a finite element adaptive strategy for the Reissner-Hellinger thermo–elasticity formulation, focusing in applications with incompressible materials. The mixed formulations are an alternative to the reduced integration techniques for facing the locking phenomenon that happens in some models of elastoplastic materials complying the Von Mises or Tresca for yield criteria and in elasticity for incompressible materials[1,2,3,4]. In such cases, if the interpolation functions are not suitably chosen, the locking characteristics might lead to failure of the finite element method. This paper will not discuss this aspect in details, but it is worth mentioning that this is the main motivation for choosing the mixed formulation and proposing new finite elements that properly deal with the volume-preserving constraint which is present in incompressible elasticity. These elements, herein proposed for thermo–elasticity, come from large experience with them in J_2-plasticity, particulary, in limit analysis applications[2].

The concepts and assumptions used in the definition of the general principles that govern the behavior of isotropic bodies, constituted of thermo-elastic material and subjected to quasi-static loads, are described in Section **2**.

In Section **3** the variational principles to describe the infinitesimal thermo–elasticity problems are proposed. One can see that the field solution of the equation system, defined by equilibrium, kinematics and constitutive equations, are optimality conditions of an $inf-sup$ mixed variational principle.

Based on space discretization generated by the finite element method, Section **4** will show the models proposed for the mixed principles which were presented in Section **3**. Triangular finite elements with quadratic and continuous interpolations for displacements and discontinuous interpolations for stress are proposed. For the stress field two different interpolations are considered. For plane stress condition, total stress is linearly interpolated. Likewise, the deviatoric stress is regarded as linear for plane strain and under symmetry of revolution conditions but the mean stress is considered to be constant in each element.

It is worthwhile to say that, regardless mixed primitive characteristics of the continuous formulation, the final discrete models can be cast in a mathematical form which is equal to that one obtained when the ordinary kinematical variational formulation is adopted as primal[2]. Section **4** shows that the viability of this process is an immediate consequence of the proposed inter–element stress discontinuities.

The proposed error indicator is based on second-order derivatives of the Mises equivalent stress and mean stress. That is, gradients and/or Hessians of the Mises equivalent stress and mean stress solutions, obtained on a given mesh, are smoothed and then used in the error estimation. The proposed estimator is focused on recovering the Hessian with a higher order of accuracy than that naturally obtained from the finite element approximation. This better approximation can be obtained by using smoothing technique associated with the finite element analysis, that is, the derivative continuity is recovered

by a process consisting of turning the inter-elements discontinuous field into a continuous one. One should highlight the importance of having low cost computational algorithms for the recovering procedure.

The error estimators will be discussed in Section **5**. Two different forms of error assessment will be presented. First, the error is estimated through the residual of the equilibrium equations over the domain, along the contour element and through the residual of the constitutive equation. These equations appear as natural conditions for the proposed mixed formulation. Finally, based on the first and second derivative recovery of the equivalent Mises stress and of the mean stress, an error indicator is proposed. An adaptive analysis based on these error estimators are presented in Section **6**.

In Section **7** two numerical application are presented. The first one aims to show the viability and capacity of this mixed formulation to face the locking phenomenon in incompressible materials. The adaptive mesh refinement performed in the second application allows one to compare the performance of the proposed error estimators with classical one.

2 GENERAL PRINCIPLES

This section presents the concepts and assumptions which are used in the definitions of the general principles that govern the behavior of isotropic bodies, constituted of thermo–elastic material and subjected to quasi-static loads.

2.1 Kinematics and Equilibrium

Consider a body occupying an open bounded region $\mathcal{B}$ with a regular boundary Γ. Let V denote the function space of all admissible displacement fields $\mathbf{u}$, sufficiently regular, complying with boundary conditions prescribed on a part Γ_u of Γ.

The strain tensor fields $\mathbf{E}$ are elements of the function space W and the tangent deformation linear operator $\mathcal{D}$ maps V onto W

$$\mathbf{E} = \mathcal{D}\,\mathbf{u} \qquad \forall\,\mathbf{u} \in V \tag{1}$$

Let $W^{'}$ be the space of stress fields $\mathbf{T}$. The internal power for any pair $\mathbf{T} \in W^{'}$ and $\mathbf{E} \in W$ is defined by the duality product

$$\big\langle \mathbf{T}, \mathbf{E} \big\rangle = \int_{\mathcal{B}} \mathbf{T} \cdot \mathbf{E}\; d\mathcal{B} \tag{2}$$

Likewise, $V^{'}$ is the space of loads and the external power dissipated by a loads system $\mathbf{F} \in V^{'}$ on a displacement field $\mathbf{u} \in V$ is given by the duality product

$$\big\langle \mathbf{F}\,,\,\mathbf{u} \big\rangle = \int_{\mathcal{B}} \mathbf{b} \cdot \mathbf{u}\; d\mathcal{B} + \int_{\Gamma_\tau} \mathbf{a} \cdot \mathbf{u}\; d\Gamma \tag{3}$$

where $\mathbf{b}$ and $\mathbf{a}$ are body and surface loads, respectively. Surface Γ_τ is the region of Γ where tractions are prescribed ($\Gamma = \Gamma_u \cup \Gamma_\tau$ and $\Gamma_u \cap \Gamma_\tau$ is empty).

The equilibrium condition, relating a stress field and a load system $\mathbf{F} \in V^{'}$, is imposed by the principle of virtual power

$$\left\langle \mathbf{T}, \mathcal{D}\mathbf{u}^* \right\rangle = \left\langle \mathbf{F}, \mathbf{u}^* \right\rangle \qquad \forall\, \mathbf{u}^* \in V^0 \tag{4}$$

where $V^0 = \{\mathbf{u}^* \in [H^1(\mathcal{B})]^3 \,/\, \mathbf{u}^*|_{\Gamma_u} = \mathbf{0}\}$.

2.2 Constitutive Relations

Let θ_0 be the reference temperature in a free stress body and θ its temperature at a subsequent instant. If $\Theta = \theta - \theta_0$ is small with respect to θ_0, the elastic properties and the density ρ can be considered invariable with the temperature. Additionally, for quasi-static process, the thermal process is invariant under stress variation[5].

In these conditions, the state law for a thermo-elastic material is obtained by selecting the thermodynamic potential, Ψ, dependent on the strain $\mathbf{E}$ and the temperature difference Θ. The inverse state law is derived from the complementar potential, Ψ^c, dependent on the stresses $\mathbf{T}$ and the temperature difference Θ, and obtained by the Legendre-Fenchel transformation[5,6] of Ψ. For linear and isotropic material, Ψ and Ψ^c are given by[5]

$$\Psi\left(\mathbf{E}, \Theta\right) = \int_{\mathcal{B}} \left\{ \frac{1}{2} \mathbb{D}\, \mathbf{E} \cdot \mathbf{E} - \frac{E}{(1-2\nu)}\, \mathrm{tr}(\mathbf{E}) \alpha \Theta - \frac{C_\epsilon}{2\theta_0} \Theta^2 \right\} d\mathcal{B} \tag{5}$$

$$\Psi^c\left(\mathbf{T}, \Theta\right) = \int_{\mathcal{B}} \left\{ \frac{1}{2} \mathbb{D}^{-1}\, \mathbf{T} \cdot \mathbf{T} + \alpha \Theta\, \mathrm{tr}(\mathbf{T}) + \left(\frac{3E}{(1-2\nu)} \alpha^2 + \frac{C_\epsilon}{\theta_0} \right) \frac{\Theta^2}{2} \right\} d\mathcal{B} \tag{6}$$

where

$$\mathbb{D} = \frac{E}{(1+\nu)}\, \mathbb{I} + \frac{E\,\nu}{(1+\nu)(1-2\nu)}\, (\mathbf{I} \otimes \mathbf{I}) \quad \text{and} \quad \mathbb{D}^{-1} = \frac{(1+\nu)}{E}\, \mathbb{I} - \frac{\nu}{E}\, (\mathbf{I} \otimes \mathbf{I}) \tag{7}$$

with $\mathbb{I}$ and $\mathbf{I}$ being, respectively, fourth and second order unit tensors, and tr(.) is the trace operator. The E is the Young's modulus, ν the Poisson's ratio , α the isotropic dilatation coefficient and C_ϵ the specific heat at constant strain. These parameters are considered independent of the temperature if small temperature variations ($\Theta/\theta_0 << 1$) are considered.

The state laws derived from these potentials allow us to express the linear thermoelastic constitutive relations in the way[5,6,7]

$$\mathbf{T} \in \nabla_{\mathbf{E}} \Psi\left(\mathbf{E}, \Theta\right) \qquad \Longleftrightarrow \qquad \mathbf{E} \in \nabla_{\mathbf{T}} \Psi^c(\mathbf{T}, \Theta) \tag{8}$$

where $\nabla_{\mathbf{E}}$ and $\nabla_{\mathbf{T}}$ represent the gradients with respect to $\mathbf{E}$ and $\mathbf{T}$, respectively. Based on (5), (6) and (8), one can rewrite the constitutive relations for thermo–elasticity by

$$\mathbf{T} = \mathbb{D}\,\mathbf{E} - \frac{E}{(1-2\nu)}\,\alpha\Theta\,\mathbf{I} \qquad \Longleftrightarrow \qquad \mathbf{E} = \mathbb{D}^{-1}\mathbf{T} + \alpha\Theta\mathbf{I} \tag{9}$$

Provided the temperature field, by the above thermo-elastic constitutive equation, it is possible to compute the strains and stresses due to the thermal effect.

3 MIXED VARIATIONAL PRINCIPLES

Thermo–elasticity problem consists in finding the stress and strain fields that occur in a body when it is under a load system $\mathbf{F}$, a temperature gradient Θ and displacement constraints. In turn, this problem consists in finding a stress field $\mathbf{T} \in W'$, a strain field $\mathbf{E} \in W$ and a displacement field $\mathbf{u} \in V$, such that the following equations system holds

$$\mathbf{E} = \mathcal{D}\,\mathbf{u} \qquad \forall\,\mathbf{u} \in V \tag{10}$$

$$\left\langle \mathbf{T}, \mathcal{D}\mathbf{u}^* \right\rangle = \left\langle \mathbf{F}, \mathbf{u}^* \right\rangle \qquad \forall\,\mathbf{u}^* \in V^0 \tag{11}$$

$$\mathbf{T} \in \nabla_{\mathbf{E}}\Psi\,(\mathbf{E}, \Theta) \qquad \Longleftrightarrow \qquad \mathbf{E} \in \nabla_{\mathbf{T}}\Psi^c(\mathbf{T}, \Theta) \tag{12}$$

For a tridimensional continuum, under infinitesimal strain assumption, the tangent deformation operator $\mathcal{D}$, coincides with the symmetric part of the gradient and the potentials Ψ and Ψ^c are given by (5) and (6), respectively.

In the following part, one can see that a solution for this system is also the solution for a variational principle, defined in function of the displacement and stress fields.

The field $\mathbf{T}$, solution for the system which is defined by the equations (10)–(12), is associated with the strains field by the constitutive relation (12) which is equivalent to [3],

$$\Psi(\mathbf{E}^*, \Theta) - \Psi(\mathbf{E}, \Theta) \geq \left\langle \mathbf{T}, \mathbf{E}^* - \mathbf{E} \right\rangle \qquad \forall\,\mathbf{E}^* \in W \tag{13}$$

The kinematic condition (10) and the equilibrium condition(11) are considered in (13) to obtain the Principle of Minimum Energy [1,3,4]: find $\mathbf{u} \in V$, such that

$$\widehat{\Pi}(\mathbf{u}) = \inf_{\mathbf{u}^* \in V^0} \left[\Psi(\mathcal{D}\,\mathbf{u}^*, \Theta) - \left\langle \mathbf{F}, \mathbf{u}^* \right\rangle\right] \tag{14}$$

The mixed principle is derived by considering in (14) the Legendre-Fenchel transformation [3]

$$\Psi(\mathbf{E}, \Theta) = \sup_{\mathbf{T}^* \in W'} \left[\left\langle \mathbf{T}^*, \mathbf{E} \right\rangle - \Psi^c(\mathbf{T}^*, \Theta)\right] \tag{15}$$

Considering in (14) the result obtained by the substitution of (6) in (15), leads to a mixed principle in two fields, which is denoted the Hellinger-Reissner Principle.

Find $\mathbf{u} \in V$, $\mathbf{T} \in W'$ such that

$$\widehat{\Pi}^{HR}(\mathbf{u},\mathbf{T}) = \inf_{\mathbf{u}^*\in V^0}\sup_{\mathbf{T}^{**}\in W'}\Big[-\frac{1}{2}\big\langle\mathbf{T}^{**},\mathbb{D}^{-1}\mathbf{T}^{**}\big\rangle+\big\langle\mathbf{T}^{**},\nabla^s\mathbf{u}^*\big\rangle- \\ -\big\langle\alpha\Theta,\mathrm{tr}(\mathbf{T}^{**})\big\rangle-\big\langle\mathbf{T}^{**}\mathbf{n},\bar{\mathbf{u}}\big\rangle_{\Gamma_u}-\big\langle\mathbf{F},\mathbf{u}^*\big\rangle\Big] \tag{16}$$

where $\langle .,. \rangle_{\Gamma_u}$ denotes the integral over Γ_u part of total contour Γ, where the displacements are prescribed. The vector $\mathbf{n}$ is the outward unit normal to Γ.

As already mentioned, the mixed principles are particularly important for applications in which the locking phenomenon is likely to occur. For example, in elasticity this phenomenon might happen when bodies constituted by incompressible materials are under symmetry of revolution or plane strain condition[1,2,3,4]. In that sense, the most convenient variational principles are the ones described in function of deviatoric and mean stress.

Splitting the stress into mean and deviatoric parts, with $\mathbf{T} = \mathbf{T^d} + \sigma_m\,\mathbf{I}$, and substituting it in (16), one can find the mixed principle as function of the displacement, the deviatoric stress $\mathbf{T^d}$ and the mean stress $\sigma_m = \mathrm{tr}\,\mathbf{T}/3$[7]

$$\widehat{\Pi}^{HR}(\mathbf{u},\mathbf{T^d},\sigma_m) = \inf_{\mathbf{u}^*\in V^0}\sup_{\substack{\mathbf{T^{d**}}\in\mathbf{W}'\\ \sigma_m^{**}\in\mathbf{R}}}\Bigg[-\frac{1}{2}\left\langle\frac{(1+\nu)}{E}\mathbf{T^{d**}},\mathbf{T^{d**}}\right\rangle - \\ -\left\langle\frac{3\,(1-2\nu)}{2\,E}\,(\sigma_m^{**})^2\right\rangle\;+\;\big\langle\mathbf{T^{d**}},(\nabla^s\mathbf{u}^*)^{\mathbf{d}}\big\rangle+\big\langle\sigma_m^{**}\,,\,\mathrm{div}(\mathbf{u}^*)\big\rangle- \\ -\big\langle 3\,\alpha\,\Theta\,,\,\sigma_m^{**}\big\rangle-\big\langle\mathbf{T^{d**}}\mathbf{n}\,,\,\bar{\mathbf{u}}\big\rangle_{\Gamma_u}-\big\langle\sigma_m^{**}\mathbf{n}\,,\,\bar{\mathbf{u}}\big\rangle_{\Gamma_u}-\big\langle\mathbf{F},\mathbf{u}^*\big\rangle\Bigg] \tag{17}$$

4 DISCRETE MODELS FOR MIXED FORMULATIONS

This section will show discrete models for the mixed principles presented in Section **3**, based on space discretizations generated by the finite element method.

4.1 Hellinger-Reissner Principle with Two Fields for Plane Stress

In discrete model for the plane stress condition, the comprised fields are defined by

$$\mathbf{u} = [\,u_x \quad u_y\,]^T\,,\;\mathbf{T} = [\,T_x \quad T_y \quad T_{xy}\,]^T \text{ and } \mathbf{E} = [\,E_x \quad E_y \quad E_{xy}\,]^T \tag{18}$$

where $\mathbf{u}$, $\mathbf{T}$ and $\mathbf{E}$ are vectors which represent displacement, stress and strain fields, respectively. Because of the vector representation of the tensorial fields, the identity is set as $\mathbf{I} = [1\;1\;0]^T$ and the deformation operator as

$$\mathcal{D} = \begin{bmatrix} \frac{\partial}{\partial x} & 0 \\ 0 & \frac{\partial}{\partial y} \\ \frac{\partial}{\partial y} & \frac{\partial}{\partial x} \end{bmatrix} \tag{19}$$

For the sake of simplicity, from now on, the following notation is adopted: a superimposed hat is used to distinguish variables, or parameters, of the continuum model from their discrete counterparts. Therefore, for each element $\mathcal{T}_e$ in a triangulation $\mathcal{T}$ over the domain $\mathcal{B}$, the interpolations for displacements, stresses and temperatures are defined as

$$\hat{\mathbf{u}}(\mathbf{x}) = \mathbf{N}_u(\mathbf{x})\ \mathbf{u}^e \quad , \quad \hat{\mathbf{T}}(\mathbf{x}) = \mathbf{N}_T(\mathbf{x})\ \mathbf{T}^e \quad \text{and} \quad \hat{\Theta}(\mathbf{x}) = \mathbf{N}_\theta(\mathbf{x})\boldsymbol{\Theta}^{\mathbf{e}} \tag{20}$$

where the vectors $\mathbf{u}^e$, $\mathbf{T}^e$ and $\boldsymbol{\Theta}^e$ are the interpolation parameters for the e element . The functions $\mathbf{N}_u(\mathbf{x})$ and $\mathbf{N}_T(\mathbf{x})$ are, respectively, the matrices of quadratic and linear shape functions[1,3,4]. For the temperature interpolations, in $\mathbf{N}_\theta(\mathbf{x})$, the quadratic continuous functions are used. Substituting the assumed interpolations in the mixed principle (16) one reaches its discrete version.

Find $\mathbf{u} \in \mathbb{R}^n$ and $\mathbf{T} \in \mathbb{R}^q$ such that

$$\begin{aligned} \Pi^{HR}(\mathbf{u},\mathbf{T}) = \min_{\mathbf{u}^* \in \mathbf{R}^n} \max_{\mathbf{T}^{**} \in \mathbf{R}^q} \Big[& -\frac{1}{2}\,\mathbb{D}^{-1}\,\mathbf{T}^{**}\ \cdot\ \mathbf{T}^{**} + \mathbf{T}^{**} \cdot \mathbf{B}\,\mathbf{u}^* - \\ & - \mathbf{F} \cdot \mathbf{u}^* + \mathbf{T}^{**} \cdot \mathbf{B}\,\bar{\mathbf{u}} - \ \mathbf{T}^{**} \cdot \boldsymbol{\Omega} \Big] \end{aligned} \tag{21}$$

where n is the number of degrees of freedom in displacements, assuming that all rigid motions are ruled out by prescribed kinematic constraints. Additionally, the continuity for displacements and the inter-element discontinuity for stresses are imposed by properly collecting the element vectors $\mathbf{u}^{\mathbf{e}}$ and $\mathbf{T}^{\mathbf{e}}$ in global vectors $\mathbf{u}$ and $\mathbf{T}$. Therefore, because of inter-element stress discontinuity, the stress parameter vector $\mathbf{T}$ is made up of disjoint sets corresponding to each element. Consequently, for plane stress condition $q = 3\ nel$, where nel is the total number of elements in the mesh.

The matrices $\mathbb{D}^{-1}$, $\mathbf{B}$ and the vectors $\mathbf{F}$ and $\boldsymbol{\Omega}$ are assembled from elementary contributions of

$$\begin{aligned} \mathbb{D}^{-1^e} &= \int_{\mathcal{T}_e} \mathbf{N}_T^T\, \widehat{\mathbb{D}}^{-1}\, \mathbf{N}_T\, d\mathcal{T} & \mathbf{B}^e &= \int_{\mathcal{T}_e} \mathbf{N}_T^T\, \mathcal{D}\, \mathbf{N}_u\, d\mathcal{T} \\ \mathbf{F}^e &= \int_{\mathcal{T}_e} \mathbf{N}_u^T\, \mathbf{b}\, d\mathcal{T} + \int_{\Gamma_\tau^e} \mathbf{N}_u^T\, \mathbf{a}\, d\Gamma_\tau & \boldsymbol{\Omega}^e &= \int_{\mathcal{T}_e} \alpha \mathbf{N}_T^T\, \mathbf{I}\, \mathbf{N}_\theta\, \boldsymbol{\Theta}^e d\mathcal{T} \end{aligned} \tag{22}$$

with $\widehat{\mathbb{D}}^{-1}$ given by (7).

If one calculates the first variation of (21), one should see that the solution of this $min - max$ problem is equivalent to the solution of the following system

$$\begin{aligned} \mathbb{D}^{-1}\,\mathbf{T} - \mathbf{B}\,\mathbf{u} - \mathbf{B}\,\bar{\mathbf{u}} + \boldsymbol{\Omega} &= \mathbf{0} \\ \mathbf{B}^T\mathbf{T} - \mathbf{F} &= \mathbf{0} \end{aligned} \tag{23}$$

4.2 Hellinger-Reissner Principle with Three Fields for Plane Strain and Symmetry of Revolution

The fields used for discretizing the symmetry of revolution and plane strain models are

$$\mathbf{u} = [\, u_x \; u_y \,]^T \,,\; \mathbf{T^d} = [\, T_x^d \; T_y^d \; T_z^d \; \sqrt{2}\,T_{xy}^d \,]^T \;\text{ and }\; \mathbf{E^d} = [\, E_x^d \; E_y^d \; E_z^d \; E_{xy}^d/\sqrt{2} \,]^T \tag{24}$$

where for symmetry of revolution $x = r,\; y = z,\; z = \theta$, with $d\mathcal{T}_e = 2\,\pi\, r\, dr\, dz$.

In this representation, the identity operator is defined by $\mathbf{I} = [\,1 \;\; 1 \;\; 1 \;\; 0\,]^T$ and the deviatoric deformation operator $\mathcal{D}^d$ and the divergent operator $\mathcal{D}_m$ can be written as

$$\mathcal{D}^d = \begin{bmatrix} \frac{2}{3}\frac{\partial}{\partial x} - \frac{1}{3}\frac{1}{x} & -\frac{1}{3}\frac{\partial}{\partial y} \\ -\frac{1}{3}\frac{\partial}{\partial x} - \frac{1}{3}\frac{1}{x} & \frac{2}{3}\frac{\partial}{\partial y} \\ -\frac{1}{3}\frac{\partial}{\partial x} + \frac{2}{3}\frac{1}{x} & -\frac{1}{3}\frac{\partial}{\partial y} \\ \frac{1}{\sqrt{2}}\frac{\partial}{\partial y} & \frac{1}{\sqrt{2}}\frac{\partial}{\partial x} \end{bmatrix} \quad \operatorname{div}\mathbf{u} = \begin{bmatrix} \dfrac{\partial}{\partial x} + \dfrac{1}{x} & \dfrac{\partial}{\partial y} \end{bmatrix} \begin{bmatrix} u_x \\ u_y \end{bmatrix} = \mathcal{D}_m\,\mathbf{u} \tag{25}$$

In $\mathcal{D}^d$ and $\mathcal{D}_m$, the terms which include factor $1/x$, should only be considered for symmetry of revolution models.

In each element, the interpolations of displacement, mean stress, deviatoric stress and temperature fields are defined by

$$\hat{\mathbf{u}}(\mathbf{x}) = \; \mathbf{N}_u(\mathbf{x})\;\mathbf{u}^e \,,\; \hat{\mathbf{T}}^{\mathbf{d}}(\mathbf{x}) = \mathbf{N}_T(\mathbf{x})\;\mathbf{T}^{\mathbf{d}^e} \,,\; \hat{\sigma}_m(\mathbf{x}) = \sigma_m^e \;\text{ and }\; \hat{\Theta}(\mathbf{x}) = \mathbf{N}_\theta(\mathbf{x})\boldsymbol{\Theta}^{\mathbf{e}} \tag{26}$$

where $\mathbf{N}_u(\mathbf{x})$, $\mathbf{N}_T(\mathbf{x})$ and $\mathbf{N}_\theta(\mathbf{x})$ are the same ones defined for the plane stress model. One should observe that the component of mean stress is interpolated piecewise constant.

Substitution of the assumed interpolation in the continuum formulation (17) leads to the following discrete counterpart

Find $\mathbf{u} \in \mathbb{R}^n$, $\mathbf{T^d} \in \mathbb{R}^q$ and $\mathbf{T_m} \in \mathbb{R}^m$ such that

$$\begin{aligned} \Pi^{HR}(\mathbf{u}, \mathbf{T^d}, \mathbf{T_m}) = \min_{\mathbf{u}^* \in \mathbf{R}^n} \max_{\substack{\mathbf{T^{d^{**}}} \in \mathbf{R}^q \\ \mathbf{T_m^{**}} \in \mathbf{R}^m}} \Bigg[& -\frac{1}{2}\,\mathbb{D}_{\mathbf{d}}^{-1}\,\mathbf{T^{d^{**}}} \cdot \mathbf{T^{d^{**}}} - \frac{1}{2}\,\mathbb{D}_{\mathbf{m}}^{-1}\,\mathbf{T_m^{**}} \cdot \mathbf{T_m^{**}} + \\ & + \mathbf{T^{d^{**}}} \cdot \mathbf{B_d}\,\mathbf{u}^* + \mathbf{T_m^{**}} \cdot \mathbf{B_m}\,\mathbf{u}^* + \mathbf{T^{d^{**}}} \cdot \mathbf{B_d}\,\bar{\mathbf{u}} + \mathbf{T_m^{**}} \cdot \mathbf{B_m}\,\bar{\mathbf{u}} - \overline{\boldsymbol{\Omega}} \cdot \mathbf{T_m^{**}} - \mathbf{F} \cdot \mathbf{u}^* \Bigg] \end{aligned} \tag{27}$$

Here, also due to proposed inter-element discontinuity for the deviatoric stresses, the parameter $q = 4\,nel$. The m-dimensional vector $\mathbf{T_m}$ collects the mean stresses of the elements, consequently the dimension m coincides with the number of the elements used in the domain discretization (nel). The matrices $\mathbb{D}_{\mathbf{d}}^{-1}$, $\mathbf{B_d}$, $\mathbf{B_m}$ and the vectors $\mathbb{D}_{\mathbf{m}}^{-1}$, $\mathbf{F}$ and $\overline{\mathbf{\Omega}}$ are adequate assemblages from elementary contributions of

$$\begin{aligned}
\mathbb{D}_{\mathbf{d}}^{-1^e} &= \int_{\mathcal{T}_e} \frac{1+\nu}{E}\, {\mathbf{N}_T}^T\, \mathbf{N}_T\, d\mathcal{T} & \mathbb{D}_{\mathbf{m}}^{-1^e} &= \int_{\mathcal{T}_e} \frac{3-6\,\nu}{E}\, d\mathcal{T} \\
{\mathbf{B}_\mathbf{d}}^e &= \int_{\mathcal{T}_e} \mathbf{N}_T^T\, \mathcal{D}^d\, \mathbf{N}_u\, d\mathcal{T} & {\mathbf{B}_\mathbf{m}}^e &= \int_{\mathcal{T}_e} \mathcal{D}_m \mathbf{N}_u\, d\mathcal{T} \\
\overline{\mathbf{\Omega}}^e &= \int_{\mathcal{T}_e} 3\alpha \mathbf{N}_\theta \Theta^e d\mathcal{T} & \mathbf{F}^e &= \int_{\mathcal{T}_e} \mathbf{N}_u^T\, \mathbf{b}\, d\mathcal{T} + \int_{\Gamma_\tau^e} \mathbf{N}_u^T\, \mathbf{a}\, d\Gamma_\tau
\end{aligned} \tag{28}$$

The solution of the $min-max$ problem (27) is equivalent to the solution of the following equations system

$$\begin{aligned}
&\mathbb{D}_{\mathbf{d}}^{-1}\mathbf{T^d} - \mathbf{B_d u} - \mathbf{B_d}\bar{\mathbf{u}} = \mathbf{0} \\
&\mathbb{D}_{\mathbf{m}}^{-1}\mathbf{T_m} - \mathbf{B_m u} - \mathbf{B_m}\bar{\mathbf{u}} + \overline{\mathbf{\Omega}} = \mathbf{0} \\
&{\mathbf{B_d}}^T\mathbf{T^d} + {\mathbf{B_m}}^T\mathbf{T_m} - \mathbf{F} = \mathbf{0}
\end{aligned} \tag{29}$$

4.3 Solution of the Discrete Models

The systems (23) and (29) do not have the ordinary mathematic structure of the finite element models for the linear elastic analysis[1,3], that is

$$\mathbf{K u} = \overline{\mathbf{F}} \tag{30}$$

Hence, in order to insert the present system in the general framework of finite element method, it is necessary to transform the system by the elimination of the stresses parameters. Because each global stress parameter is associated with a single finite element, this operation only involves quantities and operations concerning one finite element at a time. Consequently, matrix $\mathbf{K}$ and vector $\overline{\mathbf{F}}$ are obtained by assembling the elementary contribution of the following matrices

$$\mathbf{K}^e = \mathbf{B}^{eT}\, \mathbb{D}^e\, \mathbf{B}^e \qquad \overline{\mathbf{F}}^e = \mathbf{F}^e + \mathbf{B}^{eT}\, \mathbb{D}^e\, \mathbf{\Omega}^e - \mathbf{B}^{eT}\, \mathbb{D}^e\, \mathbf{B}^e \bar{\mathbf{u}}^e \tag{31}$$

for the system of (23). And for the system of (29)

$$\begin{aligned}
\mathbf{K}^e =& {\mathbf{B_d}}^{eT}\, \mathbb{D}_{\mathbf{d}}{}^e\, \mathbf{B_d}^e + {\mathbf{B_m}}^{eT}\, \mathbb{D}_{\mathbf{m}}{}^e\, \mathbf{B_m}^e \\
\overline{\mathbf{F}}^e =& \mathbf{F}^e + {\mathbf{B_m}}^{eT}\, \mathbb{D}_{\mathbf{m}}{}^e\, \overline{\mathbf{\Omega}}^e - {\mathbf{B_d}}^{eT}\, \mathbb{D}_{\mathbf{d}}{}^e\, \mathbf{B_d}^e \bar{\mathbf{u}}^e - {\mathbf{B_m}}^{eT}\, \mathbb{D}_{\mathbf{m}}{}^e\, \mathbf{B_m}^e \bar{\mathbf{u}}^e
\end{aligned} \tag{32}$$

The fact that stresses elimination is not performed under the global system is mandatory for the element computational viability. This operation envolves the inversion of the matrices $\mathbb{D}^{-1}$, $\mathbb{D}_{\mathbf{d}}^{-1}$ and $\mathbb{D}_{\mathbf{m}}^{-1}$ that, because of the stresses uncoupling, can be processed for the elementary matrices and not for the global ones.

The $\mathbb{D}^{-1^e}$ matrix is composed of two disjoint square blocks, that is

$$\mathbb{D}^{-1^e} = \begin{bmatrix} \frac{1}{E}\,\mathbf{A}^{-1} & \frac{-\nu}{E}\,\mathbf{A}^{-1} & \mathbf{0} \\ \frac{-\nu}{E}\,\mathbf{A}^{-1} & \frac{1}{E}\,\mathbf{A}^{-1} & \mathbf{0} \\ \mathbf{0} & \mathbf{0} & \frac{2+2\,\nu}{E}\,\mathbf{A}^{-1} \end{bmatrix} \tag{33}$$

where the $\mathbf{A}$ is a 3 x 3 matrix, whose components are given by $A_{ij}^{-1} = \int_{\mathcal{T}_e} h_i h_j \, d\mathcal{T}$ $(i, j = 1, 3)$, with h_i being the lagrangean linear shape functions. Inverting (33) one obtains

$$\mathbb{D}^{e} = \begin{bmatrix} \frac{E}{1-\nu^2}\,\mathbf{A} & \frac{\nu\,E}{1-\nu^2}\,\mathbf{A} & \mathbf{0} \\ \frac{\nu\,E}{1-\nu^2}\,\mathbf{A} & \frac{E}{1-\nu^2}\,\mathbf{A} & \mathbf{0} \\ \mathbf{0} & \mathbf{0} & \frac{E}{2+2\,\nu}\,\mathbf{A} \end{bmatrix} \tag{34}$$

Therefore, the invert of (33) only comprises the invert matrix $\mathbf{A}^{-1}$. The same happens with the $\mathbb{D}_{\mathbf{d}}^{-1^e}$ matrix which consists in four disjoint block-diagonal of the $\mathbf{A}^{-1}$ matrix and $\mathbb{D}_{\mathbf{m}}^{-1^e}$ which is marely a scale.

5 ERROR ESTIMATORS FOR MIXED FORMULATION

This Section presents two *a posteriori* error estimators for adaptive analysis in finite elements. At first, the error is estimated through the residual in optimal natural conditions for the proposed mixed formulation,that is, the residual in the equilibrium and constitutive equations.

In the second one, based on second-order derivatives of the Mises equivalent stress and mean stress an error indicator is proposed. Such as, gradients and/or Hessians of the Mises equivalent stress and mean stress solutions, obtained on a given mesh, are smoothed and then used in the error estimation. Any ordinary method for smooth derivatives proposed in literature could be adopted. This work particulary adopts Weighted Average, Least Squares or Patch Recovering.[8,9,10]

5.1 Residual Error Estimator

The present section suggests an error estimator based on the residual in the equilibrium equations over the domain, equilibrium along the contour element and through the residual in the constitutive equations. These are the optimal natural conditions for the mixed formulation proposed in Section **4** [10,11].

Given a regular triangulation $\mathcal{T}$, over the domain $\mathcal{B}$, such that any two triangles in $\mathcal{T}$ share at most a vertex or an edge. Let an interior edge l, one denotes by $\mathcal{T}_{in}$ and $\mathcal{T}_{out}$ the two triangles share this edge and by $\mathbf{n}_l$ the vector normal to l, pointing outward T_{in}. Then one denotes by

$$[\![\mathbf{T}_h\,\mathbf{n}]\!]_l = [\mathbf{T}_h|_{out}\,\mathbf{n}_l] - [\mathbf{T}_h|_{in}\,\mathbf{n}_l] \tag{35}$$

the jump of $\mathbf{T}_h\,\mathbf{n}_l$ across l in $\mathbf{n}_l$–direction .

Let $\mathcal{E}_I$ be the set of interior edges of $\mathcal{T}$ and for an element $\mathcal{T}_e \in \mathcal{T}$, let E_T be the set of edges of $\mathcal{T}_e$. Moreover, $|\mathcal{T}_e|$ and $|l|$ denote the area of element $\mathcal{T}_e$ and the length of the edge l, respectively.

The local error η_r^e and the global error η_r estimators are defined by

$$\eta_r^e = \left[\frac{1}{E}\left(|\mathcal{T}_e|\int_{\mathcal{T}_e}\|\mathbf{R}\|\,d\mathcal{T} + \frac{1}{2}\sum_{l\in E_T}|l|\int_l\|\mathbf{J}_l\|\,dl + \int_{\mathcal{T}_e}\|\mathbf{C}\|\,d\mathcal{T}\right)\right]^{\frac{1}{2}} \tag{36}$$

$$\eta_r = \left[\sum_{\mathcal{T}_e\in\mathcal{T}}(\eta_r^e)^2\right]^{\frac{1}{2}} \tag{37}$$

where E is the elasticity Young's modulus,

$$\mathbf{R} = \mathbf{b} + \operatorname{div}\mathbf{T}_h \qquad \text{in } \mathcal{T}_e,\ \forall\,\mathcal{T}_e \in \mathcal{T} \tag{38}$$

is the residual in the local equilibrium equation at element level $\mathcal{T}_e \in \mathcal{T}$,

$$\mathbf{J}_l = \begin{cases} [\![\mathbf{T}_h\,\mathbf{n}]\!] & \forall\, l \in \mathcal{E}_I \\ 0 & \forall\, l \subset \Gamma_u \\ 2\,(\mathbf{f} - \mathbf{T}_h\,\mathbf{n}) & \forall\, l \subset \Gamma_\tau \end{cases} \tag{39}$$

is the residual in the equilibrium equation along element boundaries and

$$\mathbf{C} = \mathbf{T}_h - \mathbb{D}\nabla^s\mathbf{u}_h \qquad \text{in } \mathcal{T}_e,\ \forall\,\mathcal{T}_e \in \mathcal{T} \tag{40}$$

is the residual in the constitutive equation at element level $\mathcal{T}_e \in \mathcal{T}$.

5.2 Error Indicator

The method considered here, the gradients and/or Hessians of the solutions, obtained on a given mesh, are smoothed and then used in the error estimation. It is well known that derivatives of the approximate solution, $g_h \in U_h$ (U_h is the interpolation space), are superconvergent in some interior points of the elements. That is, in these points derivatives of the finite element solution exhibit higher accuracy than the normally expected one. Taking advantage of superconvergency, the proposed estimator is focused on recovering the Hessian with a higher order of accuracy than that naturally obtained from the finite

element approximation. Therefore, in order to obtain the proposed error estimator, it is necessary to recover the Hessian matrix from the information given by the finite element solution g_h. Almost all algorithms that are used to recover the Hessian matrix use the first derivative information. Hence, to compute the seconde derivative it is necessary to recover previously the first derivative.

One presents the interpolation error as an indicator of the approximate solution. This is an *a posteriori* error indicator for the difference between a given function g and a discrete function g_h which is a good approximation of g in the sense that

$$\|g - g_h\|_{L^2(\Omega)} \leq C \, \| \, g - \Pi \, g \, \|_{L^2(\Omega)} \tag{41}$$

with Π denoting an operator whose approximation properties are similar to the Clement interpolation operator[12]. That is, there exists a constant C such that[13]

$$\|g - g_h\|_{L^2(\Omega)} \simeq C \, \| \, \mathcal{H}_r(g(\mathbf{x}_0)) \, (\mathbf{x} - \mathbf{x}_0) \cdot (\mathbf{x} - \mathbf{x}_0) \, \|_{L^2(\Omega)} \tag{42}$$

where $\mathcal{H}_r(g(\mathbf{x}_0))$ denotes the recovered Hessian matrix. The function g_h is the obtained field from the finite element model.

For $\|\mathbf{x} - \mathbf{x}_0\|$ small enough, relation (42) shows that the interpolation error at some point $\mathbf{x}$ is governed by the behavior of the second–order derivative. The above result suggests the use of (42) as an error indicator. Since the recovered Hessian matrix is not positive definite, it cannot be taken as a metric tensor. As an alternative, the metric tensor is introduced [9,14,15]

$$\mathbf{G} = \mathbf{Q} \, \mathbf{\Lambda} \, \mathbf{Q}^T \tag{43}$$

where $\mathbf{Q}$ is the matrix of eigenvectors of the recovered Hessian matrix, the matrix $\mathbf{\Lambda} = \text{diag}\{ \, |\lambda_1|, |\lambda_2| \, \}$, and $\{|\lambda_i|, \, i = 1, 2\}$, are the absolute value of the associated eigenvalues ($|\lambda_1| \leq |\lambda_2|$).

In computing $\mathbf{G}(g_h(\mathbf{x}_0))$ two different functions g_h are considered. In one of them g_h is associated with the Mises equivalent stress and in the another one g_h is associated with the mean stress. Therefore,

$$g_h(\mathbf{x}_0) = {\sigma^{eq}}_h(\mathbf{x}_0) = \frac{3}{2} \sqrt{\mathbf{T^d_h}(\mathbf{x}_0) \cdot \mathbf{T^d_h}(\mathbf{x}_0)} \tag{44}$$

or

$$g_h(\mathbf{x}_0) = |\sigma_{mh}(\mathbf{x}_0)| \tag{45}$$

where $\mathbf{T^d_h}$ and σ_{mh} are the recovered field obtained from original stress defined by equation system (23) or (29).

Following the above ideas, Dompierre *et al* [16] introduced an error estimator associated with the size of element edges. The interpolation indicator error introduced herein is a variation of the Dompierre's one. Instead of considering an error estimator associated to the element edge length, it is proposed to use another one that provides a measure of the

second derivative contribution in each element. Considering a given finite element mesh $\mathcal{T}_e$ of the domain $\mathcal{B}$, the indicator value which corresponds to each element $\mathcal{T}_e \in \mathcal{T}$ is defined by the following expressions[16,17]

$$\eta_i^e = \max\{\eta_i^{de}, \eta_i^{me}\} \tag{46}$$

$$\eta_i^{de} = \left\{ \int_{\mathcal{T}^e} \left[\mathbf{G} \left({\sigma^{eq}}_h(\mathbf{x}_0) \right) (\mathbf{x} - \mathbf{x}_0) \cdot (\mathbf{x} - \mathbf{x}_0) \right]^2 d\mathcal{T} \right\}^{\frac{1}{2}} \tag{47}$$

$$\eta_i^{me} = \left\{ \int_{\mathcal{T}^e} \left[\mathbf{G} \left(\sigma_{mh}(\mathbf{x}_0) \right) (\mathbf{x} - \mathbf{x}_0) \cdot (\mathbf{x} - \mathbf{x}_0) \right]^2 d\mathcal{T} \right\}^{\frac{1}{2}} \tag{48}$$

where and $\mathbf{x_0}$ is the center of the element.

The global indicator η is given by

$$\eta_i = \left[\sum_{\mathcal{B}^e \in \mathcal{B}} (\eta_i^e)^2 \right]^{\frac{1}{2}} \tag{49}$$

5.2.1 Remarks about derivative recovery

Several approaches have been proposed, in the framework of the Finite Element Method, in order to recover first derivatives[8,9,10]. The Weighted Average is one among these procedures, and it is briefly summarized in the sequel.

The recovery approach quoted Weight Average consists on turning the inter-elements discontinuous field ∇g_h into a continuous field $\nabla_R g_h$. To compute the field ∇g_h, one should apply the same element basis functions used to construct the approximation g_h. Then, a weighted average of ∇g_h, computed on the elements surrounding a node N, is adopted as the value $\nabla_R g_h(\mathbf{x}_N)$ of the recovered gradient at this node ($\mathbf{x}_N$ is the coordinate of node N). The weighted average is computed using weights which are given by the inverse of the distance between the node N and the superconvergence points of the gradient (the center of the element in case of linear triangles and Gauss points near midside nodes in case of quadratic triangles[8]).

Second derivatives can also be recovered by using the same approaches for the first derivative recuperation. In fact, in order to find $\nabla_R(\nabla_R g_h)$, each component of $\nabla_R g_h$ is considered as a new field, then one can reapply the algorithm in each one of such components. The symmetric part of the approximation is retained in order to ensure the symmetry of the recovered Hessian matrix.

6 ADAPTIVE PROCEDURE

The present adaptive procedure takes into account the global error estimator, η_r, given by (37), and the global error indicator, η_i, given by (49), for each triangulation $\mathcal{T}_k$. Then,

the objective is finding a new mesh $\mathcal{T}_{k+1}$, with a given number of elements nel. This new finite element mesh is generated in the attempt of producing a uniform distribution of the interpolation error estimator over all elements.

Our remeshing algorithm is based on the advancing front technique. In this technique, the mesh generator tries to build equilateral triangles. To evaluate the parameters, we proceed as follows

(1) Compute $\eta_\bullet^e$ in each element and then the global quantity $\eta_\bullet$, where $\eta_\bullet$ is one of the error estimators previously presented in Section **5**.

(2) Given a number of elements nel in the new adapted mesh, the expected local indicator is given by

$$\eta^* = \frac{\eta_\bullet}{\sqrt{nel}} \tag{50}$$

(3) The decreasing, or increasing, rate of the element size is estimated by

$$\beta^e = \frac{1}{\delta^e} \tag{51}$$

where

$$\delta^e = \left(\frac{f\,\eta_\bullet^e}{\eta^*} \right)^{1/2} \tag{52}$$

with f being an empiric factor, that depends on the adopted element, towards the error estimator correction . For linear triangle, this value is $f = 1.3$ and $f = 1.4$ for quadratic triangle[18].

From this rate distribution β^e, computed elementwise, nodal values are then obtained. Different approaches can be selected to this end. For instance, this operation might be based on the same scheme used to compute derivative recovery. The resulting nodal rate value is denoted by $\beta(N)$.

(4) The size of the new element, to be generated at node N, is

$$h_{k+1}(N) = \beta(N)\, h_k(N) \tag{53}$$

If necessary, the threshold values for the new element size are then enforced as

$$\underline{\alpha} \cdot h_k \;\leq\; h_{k+1} \;\leq\; \overline{\alpha} \cdot h_k \;\leq\; L \tag{54}$$

where L represents the characteristic length of the domain $\mathcal{B}$. The two parameters above, $\underline{\alpha}$ and $\overline{\alpha}$, are used in order to ensure progressive mesh adaptation.

(5) The new size distribution, h_{k+1} is then uniformly scaled. Due to limitation on the value of h, the number of elements in the new adapted mesh may be different from the expected nel. To enforce the required new number of elements, the elements size h is modified as follows

$$h_{k+1} \leftarrow \sqrt{\frac{nel_{new}}{nel}} \cdot h_{k+1} \tag{55}$$

with

$$nel_{new} = \frac{4}{\sqrt{3}} \int_{\mathcal{B}} \frac{1}{h^2} \, d\mathcal{B} \tag{56}$$

The adaptive strategy described above is repeated until the interpolation error estimator in the mesh, $\mathcal{T}_k$, becomes lower than a given admissible error $\overline{\gamma}$.

7 NUMERICAL APPLICATIONS

At First, this section presents a numerical application to show the viability and capacity of this mixed element to face the locking phenomenon in nearly incompressible materials. The second application shows an adaptive mesh refinement with the two proposed error estimators and compare their performances with the classical kinematic error estimator found in literature[18].

7.1 A Thick-Walled Cylinder Under Temperature Variation

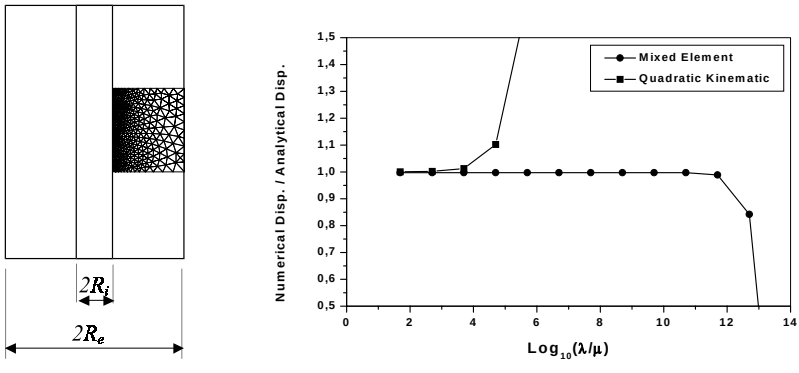

Figure 1: The finite element mesh and the behavior of the finite elements as $\nu \to 0.5$.

Let a thick-walled cylinder under temperature variation have, in the undeformed configuration, an outer radius $R_e = 5\ R_i$, where R_i is the inner radius. The temperature

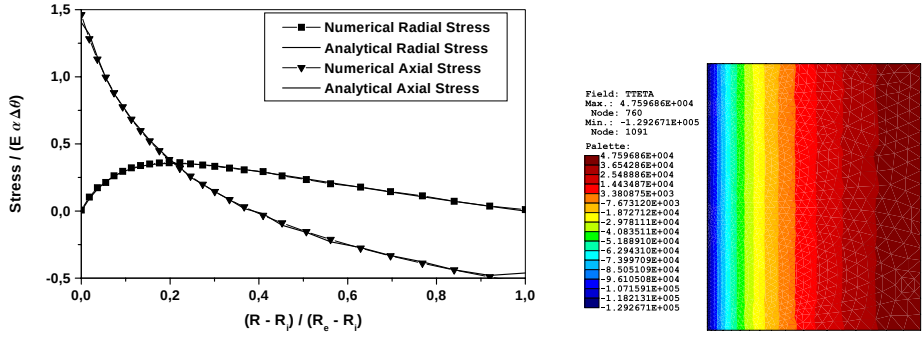

Figure 2: Graphic of the circumferential and radial stress and distribution of the circumferential stress through the thick-walled cylinder using mixed element and $\nu = 0.49999$.

variation on the inner surface of the cylinder is Θ_i and on the outer surface is Θ_e. For the stresses analysis, a mixed model with symmetry of revolution model was considered. Figure 1 shows the mesh used in this problem.

It is worthwhile to mention that here with nearly incompressible material only the mixed element had succeeded. The graphic in Figure 1 plots the ratio between the numerical and analytical displacement on the inner cylinder surface versus the logarithm of the ratio between the Lame's constants λ and μ. The parameter defined in the x-axis is an indicative of the number of "nines"used as significant digits in the definition of 0.49... as an approach for 0.5. One can observe in graphic (Figure 1) the behavior of the quadratic kinematic and mixed element proposed as Poisson's ratio approaches 0.5. The behavior of the quadratic kinematic element deteriorates in $\nu = 0.49999$. For the proposed mixed element the deterioration only commences in $\nu = 0.49999...$ (11 nines). This good behavior shows the viability and the effectiveness of the element to face the locking phenomenon.

Figure 2 presents the analytical solution for the circumferential stress field and its numerical solution which was recovered by the least square method.

7.2 A Thin Slab, With a Central Hole, Subject to Traction

A square slab with a central hole subject to uniaxial traction is considered here. Only a quarter of the slab was modelled and the ratio between the diameter d of the hole and the length l of the slab side is considered to be equal to 0.1(Figure 3).

Graphics in Figure 3 present the residual error estimator (Subsection **5.1**), the error indicator (Subsection **5.2**) and the error estimator based on the energy norm[1,3], versus the number of the elements in the adapted mesh. The convergence rate of the proposed error indicator was 1.5 and the others ones were 0.5.

Figures 4 and 5 show the evolution of the error through the adapted process, emphasizing the maximum values (in red tones) of the error in the initial step and after five

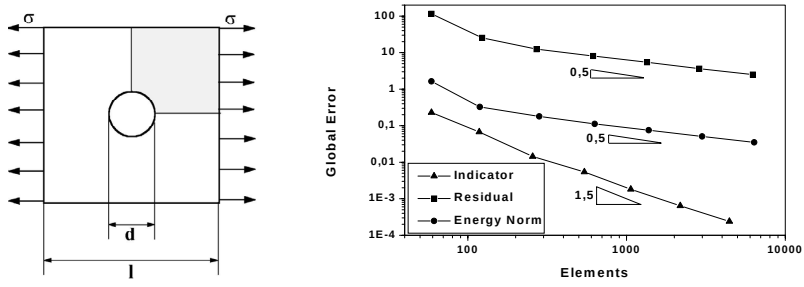

Figure 3: Model of the slab and the graphic of the error estimators behavior.

steps. The reduction and the error uniformity is evident in the adapted meshes. One can note that for the error indicator (Figure 5) there is a better uniformity of the error than of its residual error estimator (Figure 4).

In Figures 6 and 7 one can observe the evolution of the adapted mesh herein evaluated by the residual error estimator and the indicator error, respectively. For both proposed error estimators, the mesh refinement occurs in the most stress concentration place.

8 CONCLUSIONS

Models for thermo–elasticity analysis, using mixed finite elements based on the interpolation of the stress and displacement fields, were proposed. The elements are suitably indicated to facing the locking phenomenon. The element efficiency was noted in the Subsection **7.1**, in a model with symmetry of revolution, where it is known that the locking is more severe. In this case, the quadratic kinematic element did not converge for $\nu = 0.49999$, but the mixed element converged satisfactorily until $\nu = 0.4999...$ (11 nines).

Two different ways for evaluating the error of the mixed discretization were presented: first the error was estimated through the residual in the equilibrium equations over the domain along the contour of the element and through the residual in the constitutive relation. Finally, an error indicator based on second derivative recovery of the equivalent Mises stress and the mean stress was proposed. Both estimators presented a very similar behavior. It is important to emphasize that the error indicator has two advantages over the others: it is independent of the used formulation and its computational implementation is easier than others. Although similar techniques were used with this successful indicator[9] there is still the necessity of furthers studies on this matter. In the example of Subsection **7.2** one could observe that the mesh adapted presents a superior number of elements in the region where they were not supposed to be needed (right superior corner of the slab). This paper suggests that another adaptive strategy should be tested for this indicator.

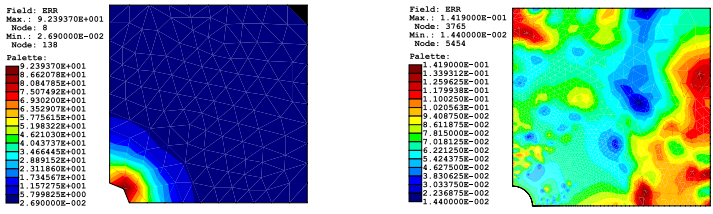

Figure 4: Distribution of the residual error estimator in the initial mesh and after five adaptive procedures.

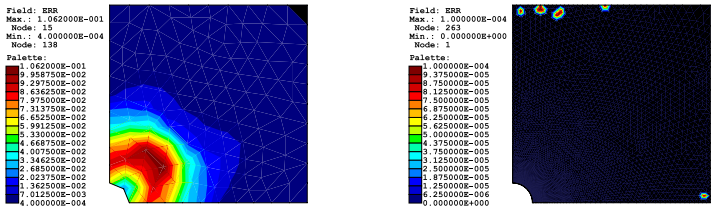

Figure 5: Distribution of the indicator error proposed in the initial mesh and after five adaptive procedures.

REFERENCES

[1] O. Zienkiewicz and R. Taylor. *The Finite Element Method*. McGraw-Hill, (1991).

[2] L.A. Borges, N. Zouain, and A.E. Huespe. A nonlinear optimization procedure for limit analysis. *European Journal of Mechanics A/Solids*, **15**, 487–512 (1995).

[3] J.R. Hughes. *The Finite Element Method - Linear Static and Dynamic Finite Elemnt Analysis*. Printice-Hall International, (1987).

[4] T. Belytschko, W.K. Liu, and B. Moran. *Nonlinear Finite Elements for Continua and Structures*. Jonh Wiley, (2000).

[5] P. Panagiotopoulos. *Inequality Problems in Mech. and Application*. Birka, (1985).

[6] J. Lemaitre and J. Chaboche. *Mechanics of Solids Materials*. Cambridge University Press, (1994).

[7] C.G. Costa and L.M.S.A. Borges. Formulação mista para termoelasticidade. 22^{nd} *Iberian Latin-American Congress on Comput. Meth. in Engng. - CILAMCE, in portuguese*, (2001).

[8] O. Zienkiewicz and J.S. Zhu. The superconvergent patch recovery and a posteriori error estimator. part 1: The recovery technique. *Int. J. Num. Meth. Engng.*, **33**, 1331–1364 (1992).

[9] L.M.S.A. Borges, N. Zouain, C.G. Costa, and R. Feijóo. An adaptive approach for limit analysis. *International Journal of Solids and Structures*, **38**, 1707–1720 (2001).

[10] C.G. Costa. Estimadores *a posteriori* baseados nas derivadas de segunda ordem. Master thesis,*in portuguese*, COPPE/PEM-UFRJ, (1999).

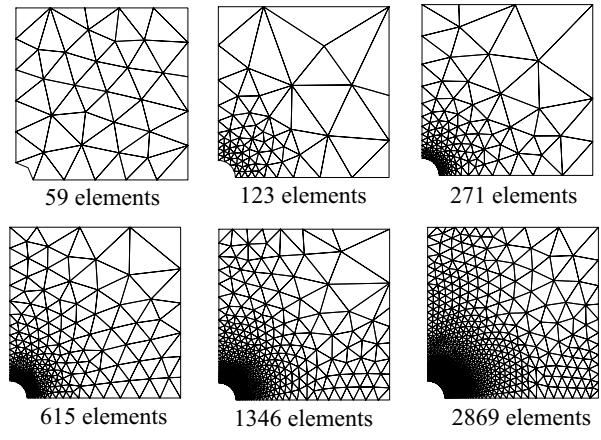

Figure 6: Adaptive mesh by residual error estimator.

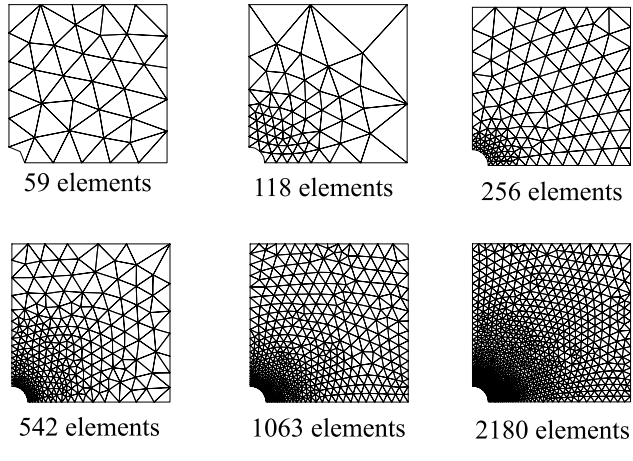

Figure 7: Adaptive mesh by error indicator.

[11] D. Braess, O. Klass, R. Niekamp, E. Stein, and F. Wobschal. Error indicators for mixed finite elements in 2-dimensional linear elasticity. *Comput. Meth. Appl. Mech. Engrg.*, **127**, 345–356 (1995).

[12] G.C. Buscaglia, R. Durán, E.A. Fancello, R.A. Feijóo, and C. Padra. An error estimator for adaptive frictionless contact finite element analysis. 4^{th} *World Congress on Comput. Mech., Buenos Aires, Argentina*, (1998).

[13] P. Clément. Approximation by finite element functions using local regularization. *RAIRO Anal. Numer.*, **R-2**, 77–84 (1975).

[14] R.C. Almeida, R.A. Feijóo, A.C.N. Galeão, C. Padra, and R. Simões. Adaptive finite element computational fluid dynamics using an anisotropic error estimator. *Comput. Mech. - New Trends and Applications. IV WCCM, Argentina*, (1998).

[15] J. Peiró. A finite element procedure for the solution of the euler equations on the unstructured meshes. Ph.d. thesis, Department of Civil Engineering, University of Swansea, UK, (1989).

[16] J. Dompierre, M.G. Vallet, M. Fortin, W.G. Habashi, D. AÏt-Ali-Yahia, S. Boivin, Y. Bourgault, and A. Tam. Edge-based mesh adaptation for cfd. *Conference on Numerical Methods for the Euler and Navier-Stokes Equations, Montreal*, (1995).

[17] R.A. Feijóo, L. Borges, and N. Zouain. Estimadores a posteriori y sus aplicaciones en el análisis adaptativo. *Technical Report, COPPE/UFRJ*, **01** (1997).

[18] O.C. Zienkiewicz and J.Z. Zhu. A simple error estimation and adaptive procedure for practical engineering analysis. *Int. J. Num. Meth. Engng.*, **24**, 333–357 (1987).